Inorganic Chemistry and Catalysis

Debye Institute for Nanomaterials

Utrecht University

Influence of Olefin- and Aromatic- Cofeed on the Carbon Deposition during Fischer-Tropsch to Olefins reaction

Bachelor Thesis

Max van Straaten

Supervisors

Lennart Weber

Prof. K.P. de Jong

Abstract

Currently aromatic compounds are synthesized by catalytic reforming of the naptha fraction and is dependent on the crude oil reserves. A breakthrough was done by developing a promoted iron catalyst (FTO-catalyst) that was able to form lower olefins with a high olefin/paraffin- ratio from synthesis gas. More work has been done to form aromatics from synthesis gas via lower olefins (FTA) using a bifunctional catalyst that consist of an FTO-catalyst mixed with a H-ZSM-5 zeolite. However during this reaction the formation of carbon was observed, which led to a pressure buildup in the reactor. This carbon formation is unwanted and therefore further investigated in this research project.

In this study, iron-based Fischer-Tropsch catalysts promoted with sodium, sulfur and manganese were prepared. These were run under Fischer-Tropsch conditions cofeeding propene and toluene to mimic the reaction conditions during Fischer-Tropsch to Aromatics. It was found that cofeeding 1 ml/min Propene increased the carbon deposition significantly for all catalysts, with exception of the 6% Fe 0.010Na 0.010S 0.10Mn catalyst. For manganese promoted catalysts a cofeed of 1 ml/min toluene decreased the carbon deposition. From the TGA data it was found that the carbon deposition possessed 3 carbon species, which can be assigned to amorphous carbon, carbon filaments and graphitic carbon. Feeding CO without olefin or aromatic cofeed had carbon filaments as the main carbon deposit, 65.8%, followed by amorphous carbon, 20.3%, and lastly graphitic carbon with 13.9%. Cofeeding olefins slightly increased the amount of graphitic carbon, percentagewise. Cofeeding Toluene however increased the percentage of carbon filaments to 81.4% whilst decreasing both amorphous and graphitic carbon percentages. It was also found that a manganese promoter in combination with Toluene cofeed inhibited the production of graphitic carbon.

Contents

Introduction 4
Fischer-Tropsch Synthesis 4
Iron-based Fischer-Tropsch catalysts 4
Promoter effect 5
Research aim 5
Literature overview 6
Fischer-Tropsch synthesis 6
Catalyst Preparation 8
Incipient wetness impregnation 8
Catalyst Characterization 8
Inductively coupled plasma mass spectrometry 8
Thermal gravimetric analysis 9
Gas chromatography 10
Experimental 11
Catalyst preparation 11
Catalytic testing 13
Post reaction analysis 14
TGA 14
Results and Discussion 15
ICP-MS 15
Catalytic performance 16
Analysis of spent catalyst 19
TGA 20
Conclusion 24
Acknowledgements 25
Appendix 26
A Weighed chemicals 26
B Catalytic testing 28
References 31

Introduction

Fischer-Tropsch Synthesis

Currently aromatic compounds are synthesized by catalytic reforming of the naptha fraction and is dependent on the crude oil reserves [1]. The field of Fischer-Tropsch Synthesis (FTS), where hydrocarbons can be formed from synthesis gas, has seen much research during the last century. The hydrocarbons used for this reaction can be derived from natural gas, coal and biomass and is thus not dependent on crude oil. The Fischer-Tropsch Synthesis however produces a wide range of products (paraffins, olefins, alcohols) within a range of C_1 to C_{40}, therefore a lot of the research performed was to done on tuning the selectivity of the reaction towards specific chemicals. In 2012 a breakthrough was done by developing a promoted iron catalyst (FTO-catalyst) that was able to form lower olefins with a high olefin/paraffin- ratio [2]. Based on this, more work has been done to form aromatics from synthesis gas via lower olefins (FTA) using a bifunctional catalyst that consist of an FTO-catalyst mixed with a H-ZSM-5 zeolite. However during this reaction the formation of carbon was observed, which led to a pressure buildup in the reactor. This carbon formation is unwanted and therefore further investigated in this research project.

Iron-based Fischer-Tropsch catalysts

Iron, cobalt, nickel and ruthenium are all catalytically active in FTS. However, nickel shows undesirably high methane selectivity and is therefore used as a methanizer catalyst, while ruthenium resources are scarce and expensive, and therefore these two elements are not used for FTS. Therefore mainly iron and cobalt are industrially used. Cobalt-based FTS catalysts, because of their high intrinsic activity and stability, are used to produce longer chain hydrocarbon products [3].

Iron-based catalysts, compared with other metal catalysts, produce less methane and more olefins when the reaction if performed at temperatures higher than 573 K. This however is achieved with the addition of promoters, without these promoters iron produces more methane. Additionally, iron-based catalysts have a high water-gas shift (WGS) activity and a higher resistance to the impurities present in syngas than the other metal catalysts [4].

Iron-based catalysts have shown high activities and light olefins selectivities with a low methane production and an excellent mechanical and chemical stability [2,5]. These results were shown using a support material, which has lower surface areas and less distribution of promoters.

Promoter effect

Commonly used promoters for iron-based Fischer-Tropsch to olefin catalysts are potassium, sodium and manganese. Sulfur however is not commonly used, but a subject of research. One of the effects of sulfur species is to change the hydrocarbon selectivity, which results in increased light olefin selectivity [6]. Besides that it also inhibits the methane production, which is a key aspect in achieving more desired hydrocarbons. However it is also often associated with poisoning of the catalyst [7]. Sodium promoted iron-based catalysts have a decreased methane selectivity, favor chain growth propagation and increased stability [8,9]. Small amounts of Manganese as a promoter decrease the deactivation rate of the catalyst in FTS reaction, this effect was caused by catalyst surface basicity and the interdispersion of iron atoms/ions with manganese oxide. However further addition of Manganese deactivated the catalyst activity. The hydrocarbon selectivity shifted slightly towards heavy hydrocarbons as well as the increase of olefin selectivity with increasing manganese content [10].

Research aim

In this project the reaction conditions during Fischer-Tropsch to Aromatics are mimicked by cofeeding propene and toluene to investigate the influence of these chemicals on the carbon deposition. The goal is to understand the process of carbon deposition during FTO/FTA reaction to develop a catalyst with a certain stability and less tendency to form coke in the future.

Literature overview

Fischer-Tropsch synthesis

The conversion of synthesis gas, a mixture of H_2 and CO, to hydrocarbons over metal catalysts was first discovered by Sabatier and Senderens in 1902 using a nickel catalyst. In the Fischer-Tropsch reaction, CO reacts with H_2 to produce hydrocarbons, which can be described by the following equations:

$$(2n+1)\ H_2 + n\ CO \rightarrow C_nH_{2n+2} + n\ H_2O \quad (1)$$

$$2n\ H_2 + n\ CO \rightarrow C_nH_{2n} + n\ H_2O \quad (2)$$

$$2n\ H_2 + n\ CO \rightarrow C_nH_{2n}H_2O + (n-1)\ H_2O \quad (3)$$

$$CO + H_2O \leftrightarrow CO_2 + H_2 \quad (4)$$

$$2\ CO \rightarrow C + CO_2 \quad (5)$$

Equation 1 shows the production of alkanes, equation 2 the production of alkenes, equation 3 the production of oxygenates, equation 4 shows the water gas shift reaction and lastly equation 5 shows the boudouard reaction[11].

There is general agreement that during the first stages of the hydrocarbon synthesis CO adsorbs on the metal. Further hydrogenation of surface-O form water, hydrogenation of carbide forms hydrocarbons and thus makes FTS a CO hydrogenation reaction.

The product range consists of aliphatic straight-chain hydrocarbons, light and heavy waxes as well as alcohols and other oxygenated products. The distribution of the products depends on the catalyst and the temperature, pressure, and residence time. These conditions typically range between temperatures of 200-350°C and pressures of 15-40 atm [12].

The products formed generally follow the statistical hydrocarbon distribution, Anderson-Schulz-Flory distribution, which is described by equation 6 [13] and is represented in *Figure 1*.

$$\mathrm{Ln}\,(C_n/n) = n \ln \alpha + \ln [(1 - \alpha)\, 2 / \alpha] \qquad (6)$$

With Cn: weight fraction of product of carbon number;

n: number of carbon atoms;

α: probability of chain growth;

$1 - \alpha$: probability of chain termination

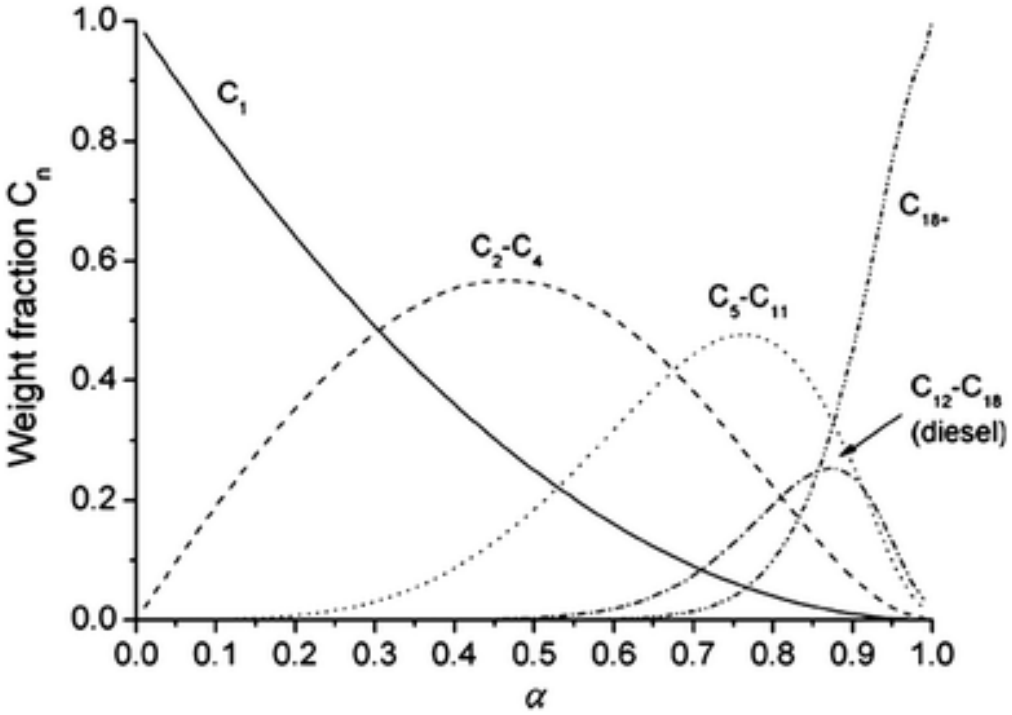

Figure 1 Anderson-Schulz-Flory distribution, showing the correlation between chain growth probability (α) and weight fraction of hydrocarbons of chain length n [14].

Catalyst Preparation

Incipient wetness impregnation

Incipient wetness impregnation is a procedure in which the required amount of elements are introduced in the volume corresponding to the pore volume of the support material. This method can be used when the species interact weakly with the surface, and for deposition of quantities that exceed the number of adsorption sites on the surface [15]. In this studies the method was used to prepare the selected catalysts.

Catalyst Characterization

Inductively coupled plasma mass spectrometry

Inductively coupled plasma mass spectrometry combines a high-temperature ICP source with a mass spectrometer. The ICP source converts the elements in the sample into ions, which are then separated and detected by the mass spectrometer. *Figure 2* shows a schematic representation of the ICP-MS. Argon gas flows inside the concentric channels of the ICP torch. The RF load coil is connected to a radio-frequency (RF) generator. As power is supplied to the load coil from the generator, oscillating electric and magnetic fields are established at the end of the torch[16]. ICP-MS is an analytical tool which can be used to detect and measure most elements on the periodic table. This analytical technique was used to characterize our prepared catalysts, in order to confirm the desired iron and promoter loading.

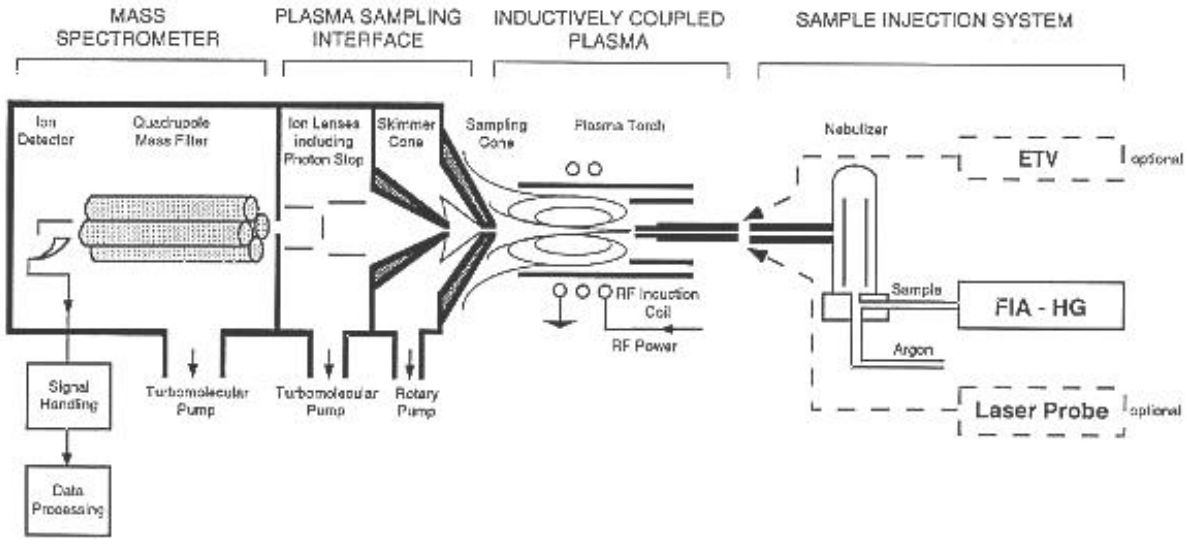

Figure 2 Schematic representation of an ICP-MS.

Thermal gravimetric analysis

Thermogravimetric analysis measures the change of mass, which is caused by decomposition/oxidation, of a sample on heating. The measurements are carried out using a thermobalance. The thermobalance consists of an electronic microbalance, a temperature-programmable furnace, and a controller, see *Figure 3*. The latter enables the sample to be simultaneously heated and weighed. The sample is weighed into a holder, which is first tared, and then suspended into the furnace. Typically a heating scheme consists of linearly increasing the temperature, but more advanced heating schemes can also be used. The balance and furnace are situated within an enclosed system so that the atmosphere can be controlled.

Thermogravimetric analysis is an important tool for desorption, decomposition, dehydration and oxidation studies[17]. In this work it will be used to determine the combustion of the carbon deposition on the spent catalysts. This information might clarify which carbon species are present on the spent catalysts.

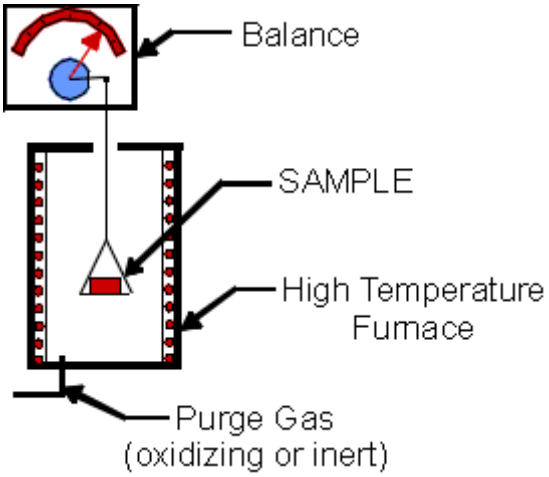

Figure 3 Schematic overview of a thermobalance [18].

Gas chromatography

Gas chromatography is an analytical tool used for separating and analyzing compounds that can vaporize without decomposition. The sample is injected, in this work using a 6-port valve, online injection and a gas phase sample, into the GC and run through a column with the flow of a carrier gas. The sample will be distributed by the use of two phases: a stationary phase and a mobile phase. The mobile phase consists of the gas flowing through the column. The stationary phase is either a solid adsorbant, or a liquid on an inert support, often located at the wall of the column, see *Figure 4*. The column can be heated during the process if desired, so the compounds stay vaporized[19]. Each compound has a retention time, which is based on the interaction with the stationary phase. This technique will be used in this research project to track the product composition during Fischer-Tropsch synthesis and also to monitor the product formation rates, which will be used to calculate the CO conversion rates.

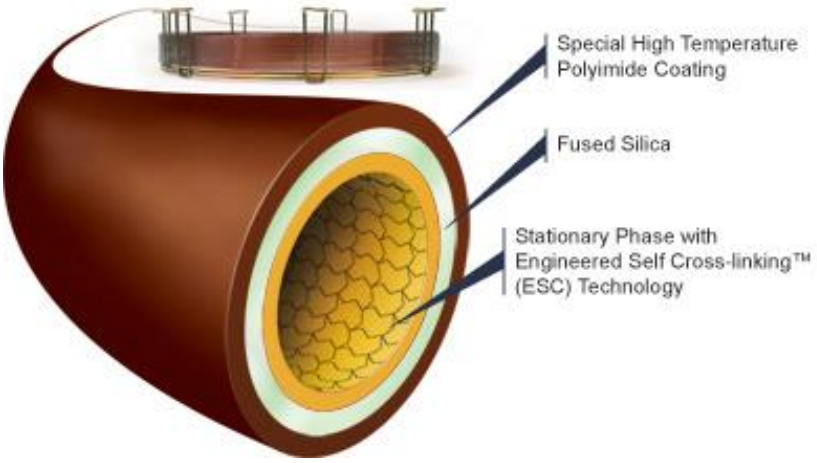

Figure 4 Schematic overview of a GC column [19].

Experimental

Catalyst preparation

In this project several iron-based catalysts were prepared using the experiments described below. These iron-based catalysts were all supported on *α*-Al_2O_3 and were aimed to have an iron weight percentage of 6. Ten catalysts were prepared with different amounts of promoters, these catalysts are listed in *Table 1*.

Catalyst	Fe	Na/Fe	S/Fe	Mn/Fe
	wt-%	atomic ratio	atomic ratio	atomic ratio
6% Fe, 0.010Na, 0.010S	6,0	0,010	0,010	-
6% Fe, 0.010Na, 0.015S	6,0	0,010	0,015	-
6% Fe, 0.010Na, 0.020S	6,0	0,010	0,020	-
6% Fe, 0.005Na, 0.010S	6,0	0,005	0,010	-
6% Fe, 0.010S, 0.050Mn	6,0	-	0,010	0,050
6% Fe, 0.010S, 0.100Mn	6,0	-	0,010	0,100
6% Fe, 0.010S, 0.150Mn	6,0	-	0,010	0,150
6% Fe, 0.010Na, 0.010S, 0.100Mn	6,0	0,010	0,010	0,100
6% Fe, 0.010Na, 0.020S, 0.100Mn	6,0	0,010	0,020	0,100
6% Fe	6,0	-	-	-

Table 1 List of prepared iron-based Fischer-Tropsch catalysts.

First step was preparation of solutions, which were used to impregnate the *α*-Al_2O_3 support. In the next paragraph a general description is given, for the values used for the different catalysts see Appendix A *Table 5.Table*

Sodium citrate tribasic dihydrate, Iron(II)sulfate heptahydrate, Ammonium iron(III) citrate and Manganese(II) nitrate tetrahydrate were dissolved in 20 mL Deionized water (DI water) in a glass jar. In some catalysts no Sodium citrate tribasic dihydrate or Manganese(II)nitrate tetrahydrate was added.

The solutions prepared were used for impregnation of the *α*-Al_2O_3 support. The corresponding amounts used for impregnation, as described in the next paragraph, can be found in Appendix A *Table 6*.

Prepared solution was added to *α*-Al_2O_3 (sieved with a 0.630mm sieve). This was done with a few droplets at a time, after which it was crushed and grinded using a pestle and mortar until it was dry again. This was repeated until half of the solution was added. Next the partially impregnated support was placed in the oven at 60°C for 20 minutes. The partially impregnated support was taken out of the oven and the other half of the solution was added. Again with a few droplets at a time followed by crushing and grinding. After all of the solution was added, the impregnated support was placed in the oven at 60°C for 60 minutes.

The catalysts were then calcined using a Nabertherm LV9/11/P330 muffle stove. The muffle stove was heated up from 25°C to 500°C in 2 hours after which it was left at 500°C during 2 more hours. Lastly it was left to cooldown to 25°C in a static atmosphere.

After calcination the catalysts were sieved to a particle size between 75 µm and 150 µm. The catalyst was first compressed using a Carver model 3853-0 with a force of 8 metric tons to obtain a pellet. This pellet was then crushed and grinded using a pestle and mortar. The catalyst was sieved to obtain the desired particle size. Samples were sent for ICP-MS to analyze the composition.

Catalytic testing

For each experiment about 30 mg of catalyst, sieved 75-150 µm, was homogeneously mixed with SiC, an inert diluent, with a dilution of 2 by volume and loaded into the fixed bed reactor. Quartz wool was added on top of the catalyst bed. The reactor was placed in an oven while a thermocouple monitored the temperature in the catalyst bed.

The reaction was run using the desired program, which is shown in *Figure 5*, for the complete table containing flow rates and temperature ramps see Appendix B *Table 7, Table 8, Table 9 and Table 10*. The measurement started by heating the oven to 350°C and holding it at this temperature for 2 hours, in which the catalyst was being reduced. Next the oven was cooled to 290°C and kept at this temperature for an hour, during this hour the iron carbides were being formed. After that the oven was heated to 400°C. It was hold at this temperature for 4.5 hours and during this time the Fischer-Tropsch to olefins reaction took place. After that the oven was cooled down and CO and H_2 were flushed out.

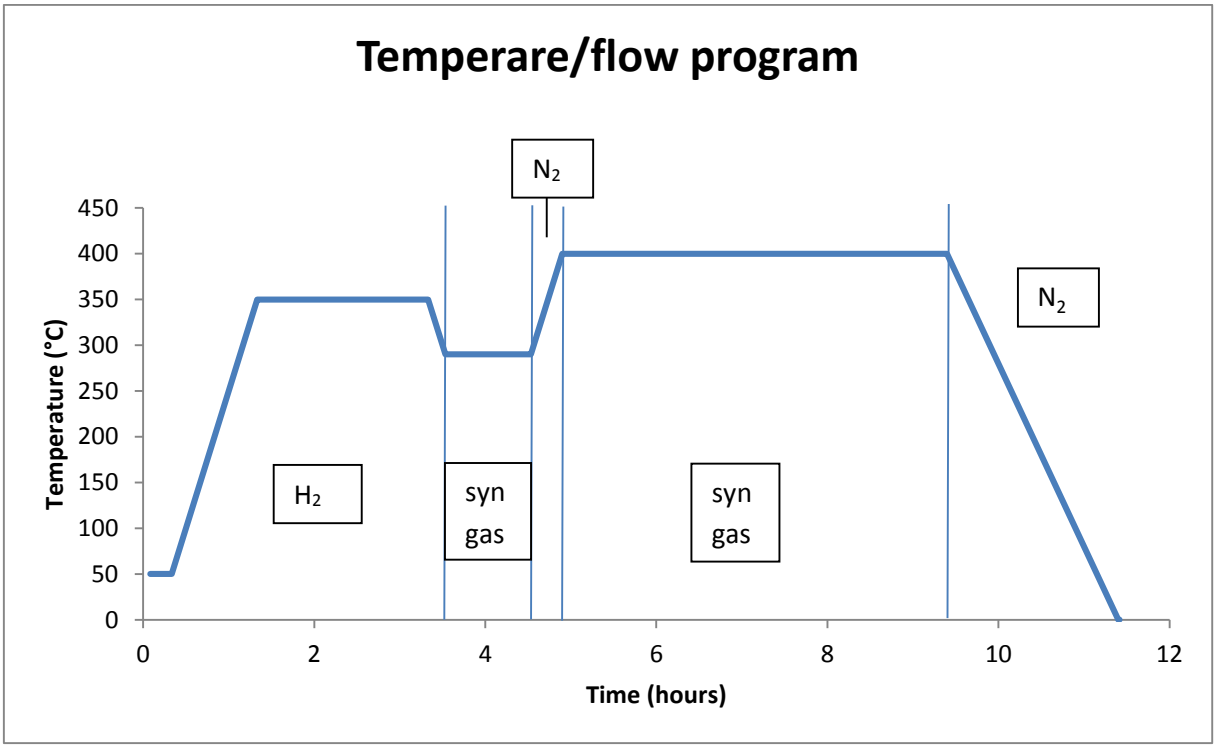

Figure 5 Flow program used for carburization and FTO reaction without a cofeed.

Post reaction analysis

The spent catalyst was removed from the fixed bed reactor and the quartz wool was removed from the spent catalyst. The catalyst was then weighed and placed in a muffle stove. The muffle stove was first heated from 25°C to 500°C during 2 hours. After that it was kept at 500°C during another 5 hours in static atmosphere. Lastly the spent catalyst was left to cooldown to 25°C again in static atmosphere. After this thermal treatment the spent catalyst was weighed again. This way the weight loss corrected for the oxidation of carbide to Fe(III)oxide can be calculated.

TGA

The spent catalysts that were analyzed using TGA were first separated from the SiC using a strong magnet. The fraction containing the spent catalyst was loaded into a platinum holder, which was first tared on the TGA. The analysis was started from 25°C and linearly heated to 1000°C with a slope of 15°C per minute. A constant gas flow of Nitrogen 40.0 ml/min and Air 60.0 ml/min was used during the measurement. The advantage of using the TGA with regards to using the muffle stove is that the weight is monitored over the temperature. And thus the TGA gives a more detailed analysis during carbon burn off.

Results and Discussion

ICP-MS

In *Table 2* the results obtained from ICP-MS analysis and the expected element composition can be found. From this data it is obvious that the ratios of Sulfur to Iron and Manganese to Iron are in line with the expectations. For the ratio of Sodium to Iron however all of the ratios are higher than expected, and even for catalyst 6% Fe, 0.010S, 0.100Mn which expected a ratio of 0.000 there still is a ratio present of 0.023. This can be explained by the fact that Ammonium iron(III) citrate, one of the precursors used, had impurities in their preparation steps.

Catalyst	Fe		Na/Fe		S/Fe		Mn/Fe	
	wt-%	wt-%	atomic ratio	atomic ratio	atomic ratio	atomic ratio	atomic ratio	atomic ratio
	ICP-MS	Expected	ICP-MS	Expected	ICP-MS	Expected	ICP-MS	Expected
6% Fe, 0.010Na, 0.010S	4,95	6,00	0,036	0,010	0,009	0,010	0,000	0,000
6% Fe, 0.010Na, 0.015S	5,67	6,00	0,032	0,010	0,013	0,015	0,000	0,000
6% Fe, 0.010Na, 0.020S	5,53	6,00	0,033	0,010	0,018	0,020	0,000	0,000
6% Fe, 0.010S, 0.100Mn	5,71	6,00	0,023	0,000	0,008	0,010	0,105	0,100
6% Fe, 0.010Na, 0.010S, 0.100Mn	5,82	6,00	0,030	0,010	0,008	0,010	0,103	0,100

Table 2 ICP-MS results and expected element composition.

Catalytic performance

The CO conversion rates were calculated using the product formation rates measured with the GC for hydrocarbons and the numbers of the hydrocarbon feed. In *Figure 6* the calculated conversion rates for the catalysts ran without cofeed are displayed. From these calculations, noteworthy is that the conversion rate of the 5% Fe, 0.010Na, 0.010S catalyst dropped drastically within 2 hours. For all of the catalysts it is evident that it took between 1 and 2 hours before a steady state was achieved.

Interesting to note is that for the catalysts without manganese an increase of CO conversion followed by a drop with increasing sulfur content. And that the 6% Fe, 0.010Na, 0.015S catalyst has the highest initial conversion rates.

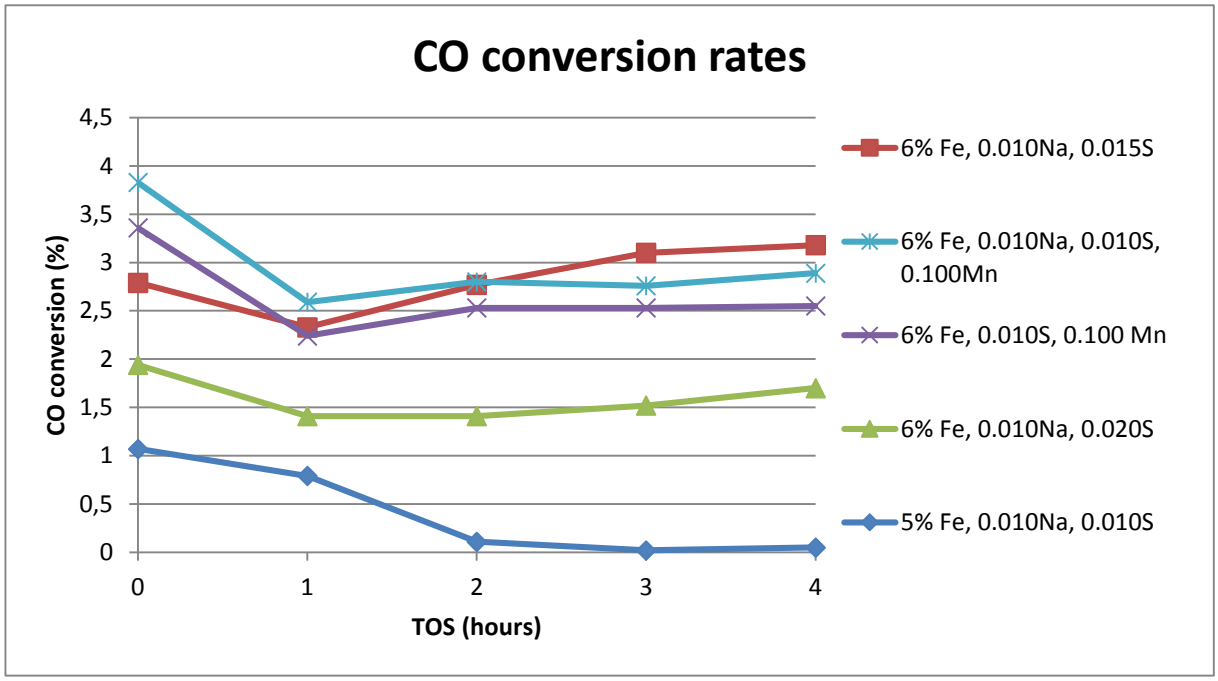

Figure 6 Calculated CO conversion rates, 400°C, 1 bar, GHSV: 7200 h-1, CO : H2 = 1

An important aspect is the olefin to paraffin ratio, seeing that the main goal is to synthesize aromatics. In *Figure 7* the olefin to paraffin ratio for the ethylene and propene fraction are displayed. It can be clearly seen that the catalysts without manganese as a promoter have higher olefin to paraffin ratios after 1 hour on stream, but they then show a steep drop in the ratios. For the manganese promoted catalysts the ratios are much lower than for the catalysts without manganese, however it is worthy to note that they appear to be stable after 2 hours on stream.

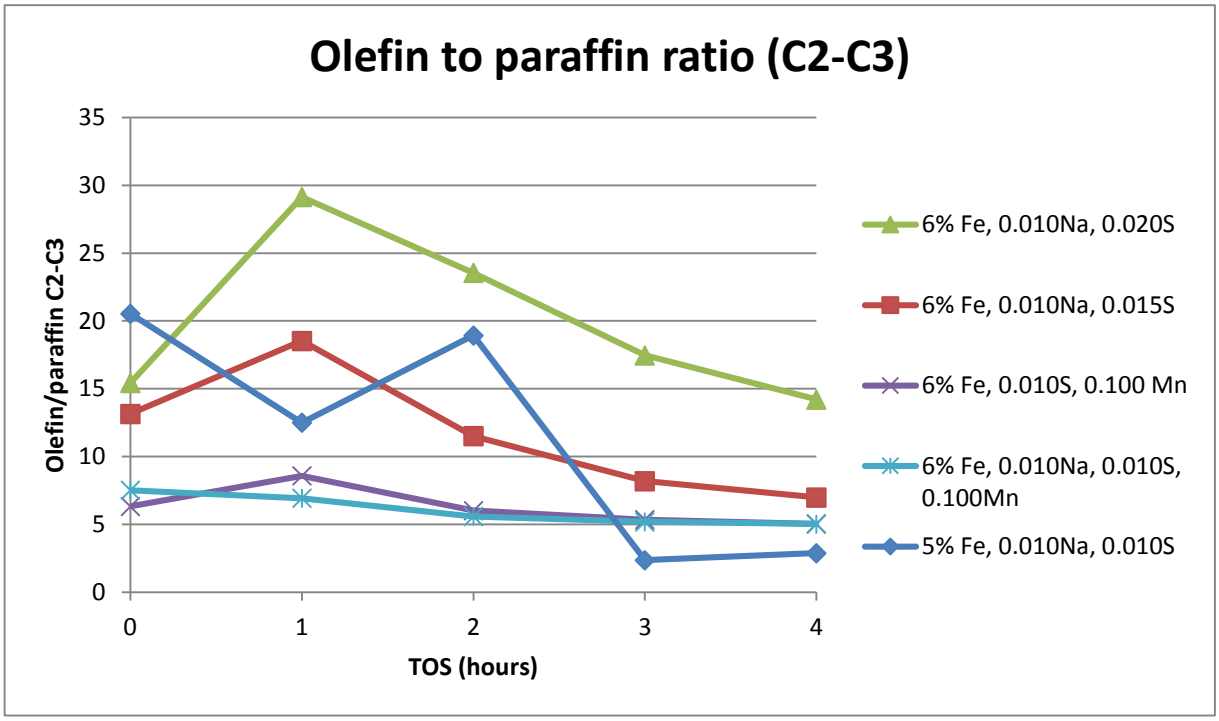

Figure 7 Olefin to paraffin ratios C2-C3, 400°C, 1 bar, GHSV: 7200 h-1, CO : H2 = 1

The methane selectivity for the iron-based Fischer-Tropsch catalysts is shown in *Figure 8.* For the 5% Fe, 0.01Na, 0.01S catalyst the selectivity goes down over time, whereas for the other 4 catalysts the selectivity to methane seems to go up. This drop should be appointed to the drastic drop in calculated CO conversion rate as observed earlier for this catalyst.

The manganese promoted catalysts seem to have a higher initial methane selectivity compared to the catalysts without manganese, but also appear to be more stable. For the 6% Fe, 0.01Na, 0.01S, 0.10Mn catalyst there even seems to be a drop in methane selectivity. For most of the catalysts, a high methane selectivity between 45-50% is calculated. The 6% Fe, 0.01Na, 0.02S has a lower methane selectivity around 40%.

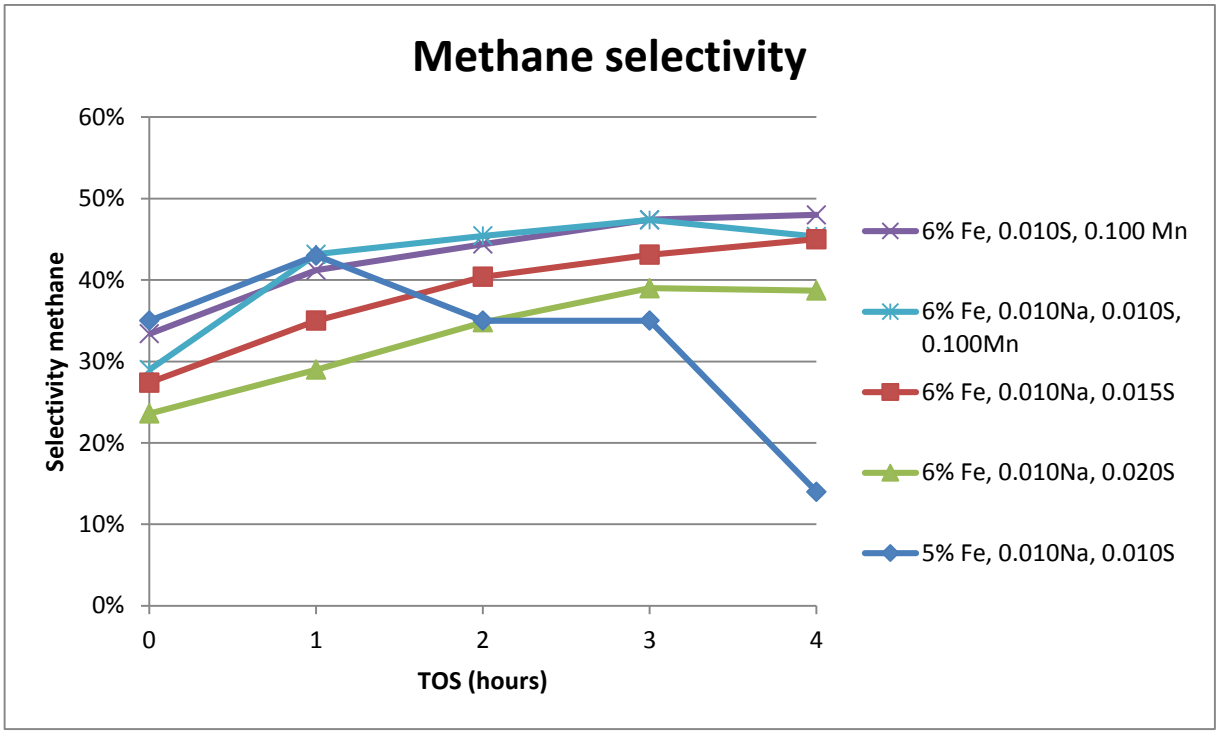

Figure 8 Methane selectivity, 400°C, 1 bar, GHSV: 7200 h-1, CO : H2 = 1

Analysis of spent catalyst

The mass loss in weight percentage of the catalytic material, the added SiC is not included in this calculation, versus the type of cofeed can be found in *Figure 9*. These results have been corrected for the weight gain caused by the oxidation of the iron carbides to iron(III)oxide assuming that the iron is fully carburized.

From the data a pattern is observed, being that for the 1 ml/min Propene cofeed all catalysts undergo an increase in total carbon deposition. For almost all, with exception of 6% Fe 0.010Na 0.010S 0.10Mn, the increase in mass loss is significant.

Even further increasing the Propene cofeed from 1 ml/min to 2ml/min however does not increase the mass loss further on for most catalyst. For 6% Fe 0.010Na 0.010S 0.10Mn there even is an decrease in mass loss. For the 5% Fe 0.010Na 0.010S catalyst there is a significant increase in mass loss, which could explain the rapid loss of calculated CO conversion rates earlier.

Another interesting trend is that when 1ml/min Toluene is cofed, the catalysts with manganese have less carbon deposition than without cofeed. Whereas the catalysts without manganese have an increase in mass loss going from no cofeed to 1ml/min Toluene cofeed.

The influence of olefin cofeed appears to increase the mass loss and could thus be important in the process of coking. For the aromatic cofeed however this does not seem to influence the coking as much as the olefin cofeed, however it does slightly increase the coke if no manganese promoters are present.

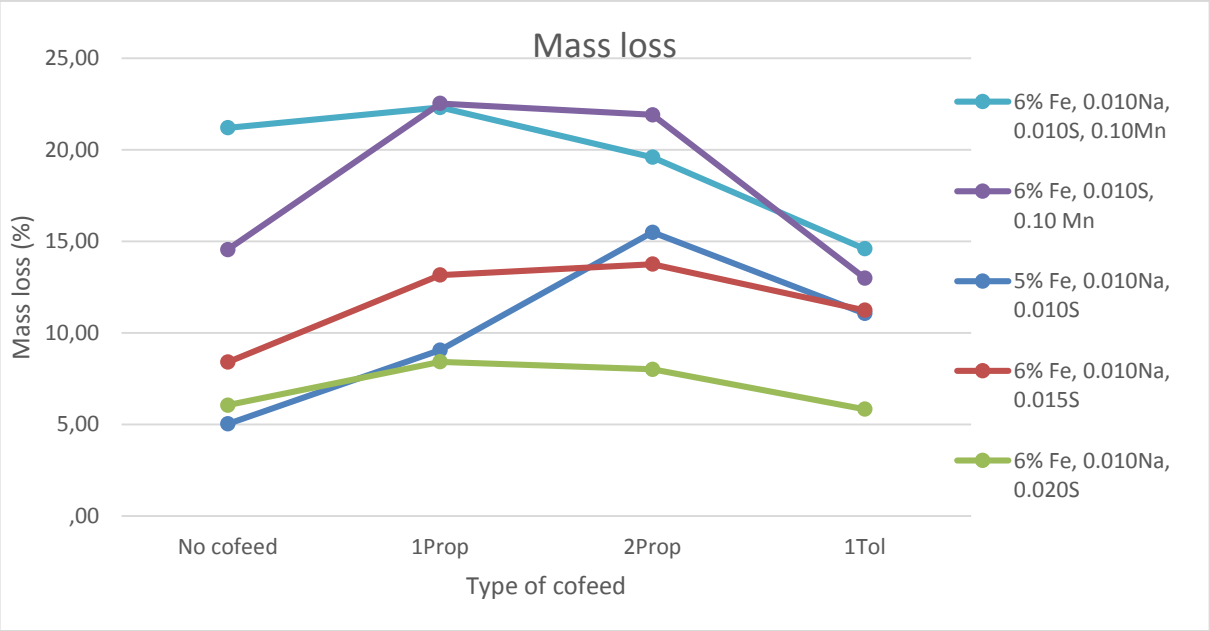

Figure 9 Mass loss plotted in weight percentage of the catalytic material versus the type of cofeed.

TGA

In *Figure 10* a typical TGA plot is shown for the derivative weight versus the temperature of the iron-based Fischer-Tropsch catalysts not promoted with manganese. In this plot there are 4 peaks, actually 5 but one is at 200°C. The negative curve at 200°C is caused by the oxidation of the iron carbides into iron(III)oxide, causing an increase in weight, and therefore a negative peak in the derivative weight. This plot suggests that there are 3 or 4 different carbonaceous species on the spent iron-based Fischer-Tropsch catalyst. When these TGA plots are compared to the literature [20,21,22] the peaks can be assigned. Left peak corresponding to amorphous carbon, middle peak to carbon filaments and the right peak to graphitic carbon.

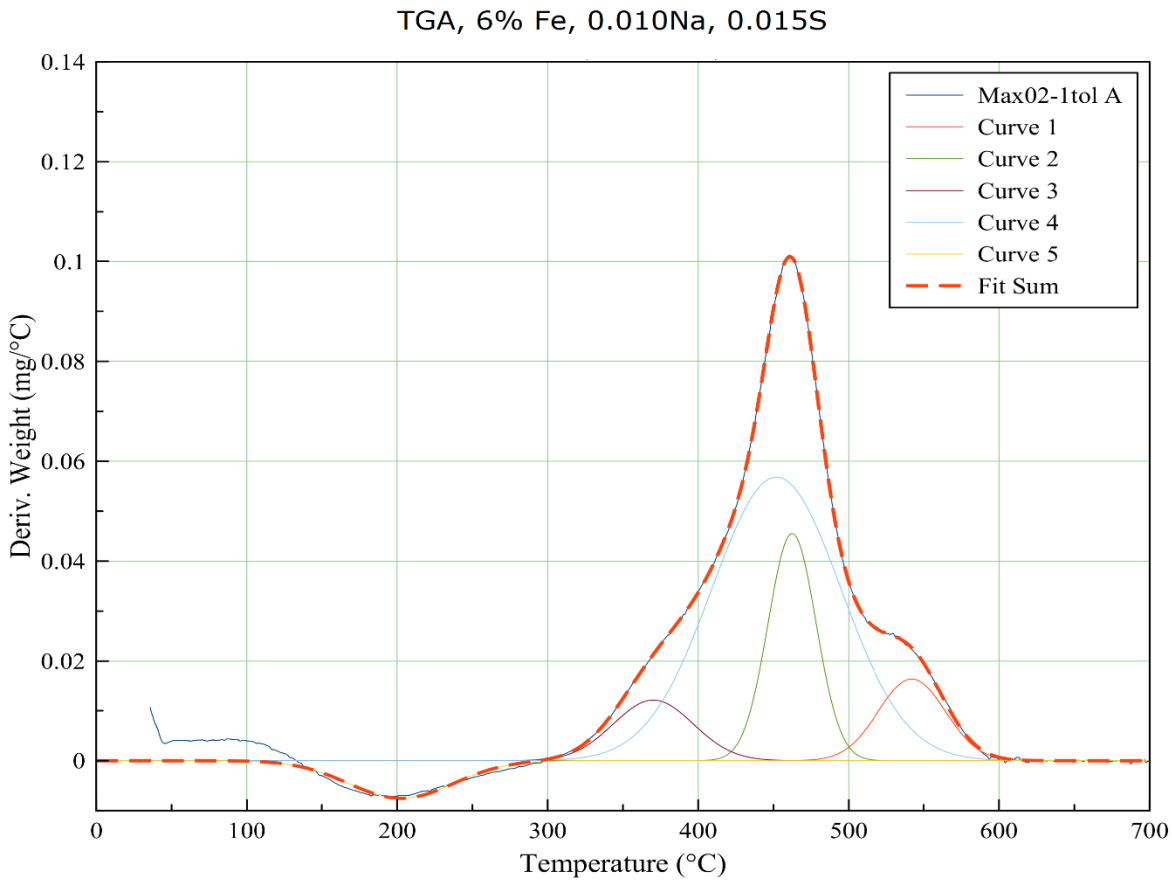

Figure 10 TGA plot for 6% Fe, 0.010Na, 0.015S

Table 3 contains the values of weight and percentages corresponding to the peaks for the 5% Fe 0.010Na 0.010S catalyst, the two carbon filament peaks in the middle have been summed, for the different kinds of cofeed. An increase of the carbon filament peaks is observed when cofeeding 1 ml/min Toluene, note the cumulative peak area is not increasing. For the other catalysts cofed with 1 ml/min Toluene this same pattern was observed, therefore Toluene seems to inhibit graphitic carbon production and increase the production of carbon filaments. Feeding CO without olefin or aromatic cofeed has carbon filaments as the main carbon deposit, 65.8%, followed by amorphous carbon, 20.3%, and lastly graphitic carbon with 13.9%. Cofeeding olefins slightly increases the amount of graphitic carbon, percentagewise, but does not significantly affect the composition. Cofeeding Toluene however increases the percentage of the middle peaks, corresponding to carbon filaments to 81.4% and decreasing both amorphous and graphitic carbon.

	Peek area						
Cofeed	Left		Middle		Right		Cumulative
	(mg)	(%)	(mg)	(%)	(mg)	(%)	(mg)
none	0,488	20,3	1,586	65,8	0,335	13,9	2,409
1ml/min prop	0,612	23,8	1,496	58,2	0,461	17,9	2,570
2ml/min prop	0,393	18,2	1,442	66,7	0,328	15,2	2,162
1ml/min tol	0,272	11,2	1,975	81,4	0,179	7,4	2,426

Table 3 Peak areas found for the different types of cofeed for 5% Fe 0.010Na 0.010S

In *Figure 11* a typical plot for the manganese promoted iron-based Fischer-Tropsch catalysts is displayed. For this plot there were only 3 peaks, 4 including the peak at 200°C which again represents the oxidation of iron carbides to iron(III)oxide. Suggesting that in this case only amorphous carbon and carbon filaments are present. If we compare the manganese promoted and non-manganese promoted Fischer-Tropsch catalyst plots, we can clearly see that for the manganese promoted plots the right most peak is not present, which corresponds to graphitic carbon.

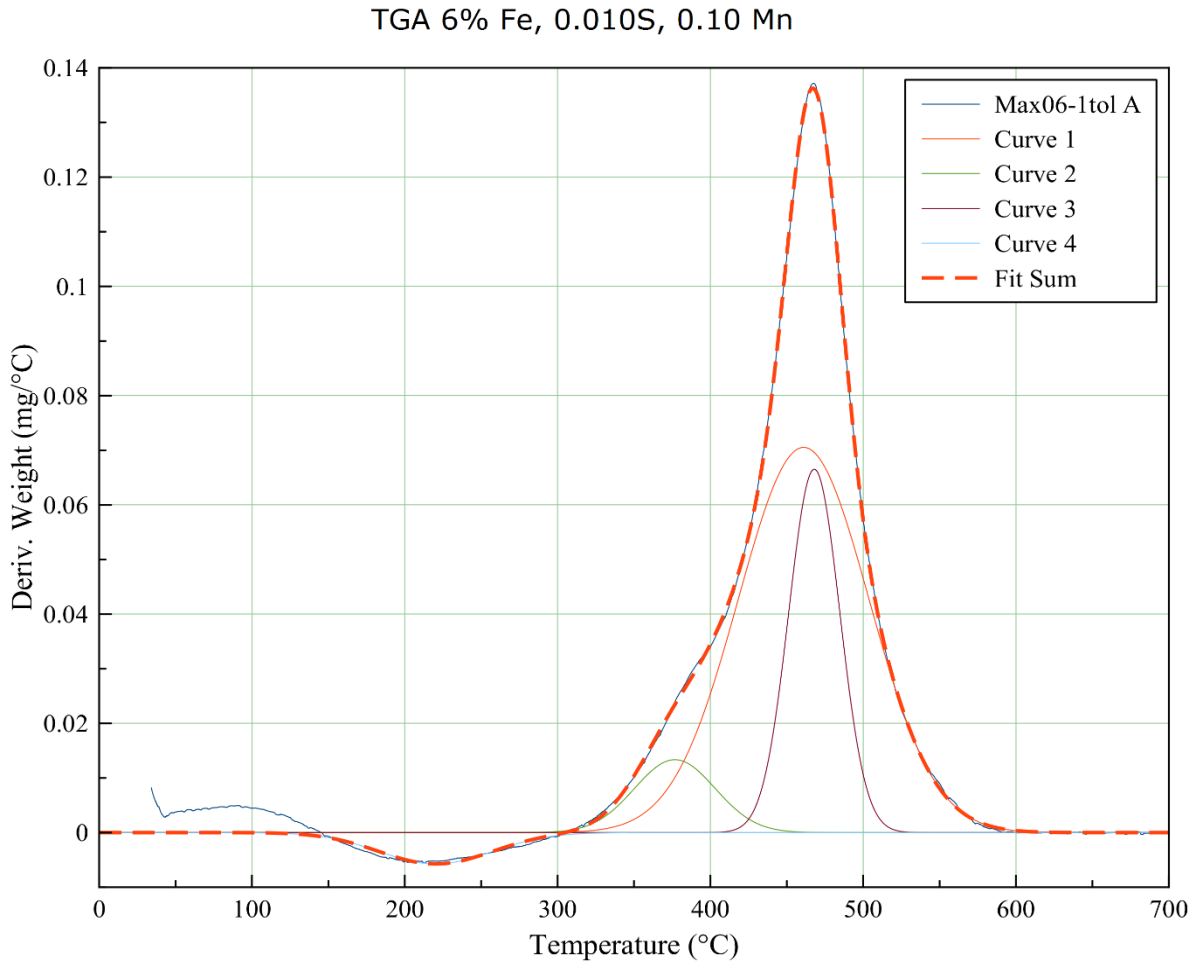

Figure 11 TGA plot for 6% Fe, 0.010S, 0.10Mn

Table 4 displays the area regions, the middle two peaks have been summed, found in the TGA plots when cofeeding 1ml/min Toluene. There is obviously a trend here, the addition of manganese promoter inhibits the production of graphitic carbon. When comparing the percentage of carbon filaments to those with different cofeed, it is evident that this percentage increases when cofeeding 1 ml/min Toluene.

Catalyst	**Peek area**						
	Left		Middle		Right		Cumulative
	(mg)	(%)	(mg)	(%)	(mg)	(%)	(mg)
5% Fe, 0.010Na, 0.010S	0,272	11,2	1,975	81,4	0,179	7,4	2,426
6% Fe, 0.010Na, 0.015S	0,165	8,4	1,619	82,2	0,186	9,5	1,970
6% Fe, 0.010Na, 0.020S	0,152	12,7	0,929	77,8	0,113	9,5	1,194
6% Fe, 0.010S, 0.10 Mn	0,183	7,9	2,150	92,1	0,000	0,0	2,334
6% Fe, 0.010Na, 0.010S, 0.10Mn	0,257	9,5	2,456	90,5	0,000	0,0	2,713

Table 4 Peak areas in mg found for the different types of promoters whilst cofeeding 1 ml/min Toluene.

Conclusion

From the ICP-MS measurements it can be concluded that the ratio of sulfur to iron and the ratio of manganese to iron were as expected. For Sodium however the ratios were higher than expected, but this can be explained by the fact that Ammonium iron(III) citrate, one of the precursors used, had impurities in their preparation steps.

From the catalytic performance it was observed that the manganese promoted catalysts had lower olefin to paraffin ratios than the catalysts without manganese promoters. The 6% Fe, 0.01Na, 0.02S had the highest olefin to paraffin ratios for both C2 and C2-C3 fractions and had the lowest methane selectivity, however the CO conversion rate for this catalyst was lower.

The analysis of spent catalysts, using methods to determine weight loss, found that cofeeding 1 ml/min Propene increases the carbon deposition for all catalysts. This increase was significant with exception of the 6% Fe 0.010Na 0.010S 0.10Mn catalyst. Further increase of the Propene feed does not further increase carbon deposition, however for 6% Fe 0.010Na 0.010S 0.10Mn there even is an decrease in mass loss. For the 5% Fe 0.010Na 0.010S catalyst there was a significant increase in carbon deposition. Another interesting trend is that when 1ml/min Toluene was cofed, the catalysts with manganese had less carbon deposition than without cofeed. Thus addition of a manganese promoter whilst cofeeding Toluene appears to decrease the carbon deposition.

The influence of olefin cofeed appears to increase the carbon deposition and could thus be important in the process of coking. For the aromatic cofeed however this does not seem to influence the coking as much as the olefin cofeed, but it does slightly increase the coking when no manganese promoters are present.

From the TGA data, it was found that the carbon deposition possessed 3 carbon species, which can be assigned to amorphous carbon, carbon filaments and graphitic carbon, in order of increasing temperature. Feeding CO without olefin or aromatic cofeed has carbon filaments as the main carbon deposit, 65.8%, followed by amorphous carbon, 20.3%, and lastly graphitic carbon with 13.9%. Cofeeding olefins slightly increased the amount of graphitic carbon, percentagewise, but did not significantly affect the composition. Cofeeding Toluene however increased the percentage of carbon filaments to 81.4% and decreased both amorphous and graphitic carbon. It was also found that a manganese promoter in combination with Toluene cofeed inhibited the production of graphitic carbon.

Acknowledgements

Tom van Deelen and Martin Oschatz have my gratitude for their week of supervision they provided.

But most importantly for my research project I would like to thank ICC and my supervisors for giving the opportunity to do my bachelor's thesis at their department and my direct supervisor Lennart Weber specifically for training me during these weeks and providing me with a lot of useful techniques and knowledge.

Appendix

A Weighed chemicals

The chemicals weighed for the prepared solutions are reported in *Table 5*, the amounts of solution and support material used for impregnation are reported in *Table 6*.

Catalyst	Sodium citrate tribasic dihydrate (mg)	Iron(II)sulfate heptahydrate (mg)	Ammonium iron(III) citrate (mg)	Manganese(II) nitrate tetrahydrate (mg)
6% Fe, 0.010Na, 0.010S	26.81	73.08	8485.90	-
6% Fe, 0.010Na, 0.015S	27.81	118.71	10479.08	-
6% Fe, 0.010Na, 0.020S	28.70	159.24	10425.73	-
6% Fe, 0.005Na, 0.010S	14.00	79.65	10534.31	-
6% Fe, 0.010S, 0.050Mn	-	79.89	10530.86	357.35
6% Fe, 0.010S, 0.100Mn	-	79.08	10532.81	721.00
6% Fe, 0.010S, 0.150Mn	-	79.69	10531.19	1073.78
6% Fe, 0.010Na, 0.010S, 0.100Mn	27.73	79.23	10541.51	716.50
6% Fe, 0.010Na, 0.020S, 0.100Mn	28.81	158.92	10425.38	718.90
6% Fe	-	-	10638.30	-

Table 5 Weighed chemicals dissolved in 20mL Deionized water.

Catalyst	*α*-Al_2O_3 Support (g)	Solution (mL)	Catalyst	*α*-Al_2O_3 Support (g)	Solution (mL)
6% Fe, 0.010Na, 0.010S	5.65	4.52	6% Fe, 0.010S, 0.100Mn	2.11	1.688
6% Fe, 0.010Na, 0.015S	1.84	1.472	6% Fe, 0.010S, 0.150Mn	1.897	15.176
6% Fe, 0.010Na, 0.020S	1.314	10.512	6% Fe, 0.010Na, 0.010S, 0.100Mn	1.718	13.744
6% Fe, 0.005Na, 0.010S	1.834	14.672	6% Fe, 0.010Na, 0.020S, 0.100Mn	1.735	1.388
6% Fe, 0.010S, 0.050Mn	1.664	13.312	6% Fe	12	9.6

Table 6 Samples with corresponding amounts of precursors used.

B Catalytic testing

Below additional information regarding the temperature program and flow programs used for the experiments can be found.

Step	Dwell	Temp	Ramp	H2	CO	N2
	(min)	(°C)	(°C /min)	(ml/min)	(ml/min)	(ml/min)
1	5	50	5	0	0	2
2	5	50	5	0	0	2
3	60	350	5	10	0	5
4	120	350	5	10	0	5
5	12	290	5	10	0	5
6	60	290	5	3	3	0
7	22	400	5	0	0	5
8	270	400	5	3	3	0
9	120	0	50	0	0	5
10	1	0	5	0	0	2

Table 7 Flow program used for carburization and FTO reaction without a cofeed.

Step	Dwell	Temp	Ramp	H2	CO	Propene	N2	Toluene
	(min)	(°C)	(°C /min)	(ml/min)	(ml/min)	(ml/min)	(ml/min)	(ml/min)
1	5	50	5	0	0	0	2	0
2	15	50	5	0	0	0	2	0
3	60	350	5	10	0	0	5	0
4	120	350	5	10	0	0	5	0
5	12	290	5	10	0	0	5	0
6	60	290	5	3	3	0	0	0
7	22	400	5	0	0	0	5	0
8	270	400	5	2,5	2,5	1	0	0
9	120	0	50	0	0	0	5	0
10	1	0	5	0	0	0	2	0

Table 8 Flow program used for carburization and FTO reaction with a cofeed of 1ml/min Propene

Step	Dwell	Temp	Ramp	H2	CO	Propene	N2	Toluene
	(min)	(°C)	(°C/min)	(ml/min)	(ml/min)	(ml/min)	(ml/min)	(ml/min)
1	5	50	5	0	0	0	2	0
2	15	50	5	0	0	0	2	0
3	60	350	5	10	0	0	5	0
4	120	350	5	10	0	0	5	0
5	12	290	5	10	0	0	5	0
6	60	290	5	3	3	0	0	0
7	22	400	5	0	0	0	5	0
8	270	400	5	2	2	2	0	0
9	120	0	50	0	0	0	5	0
10	1	0	5	0	0	0	2	0

Table 9 Flow program used for carburization and FTO reaction with a cofeed of 2ml/min Propene

Step	Dwell	Temp	Ramp	H2	CO	Propene	N2	Toluene
	(min)	(°C)	(°C/min)	(ml/min)	(ml/min)	(ml/min)	(ml/min)	(ml/min)
1	5	50	5	0	0	0	2	0
2	15	50	5	0	0	0	2	0
3	60	350	5	10	0	0	5	0
4	120	350	5	10	0	0	5	0
5	12	290	5	10	0	0	5	0
6	60	290	5	3	3	0	0	0
7	22	400	5	0	0	0	5	0
8	270	400	5	2,5	2,5	0	0	1
9	120	0	50	0	0	0	5	0
10	1	0	5	0	0	0	2	0

Table 10 Flow program used for carburization and FTO reaction with a cofeed of 1ml/min Toluene

References

[1] C. E. Slyngstad, Ind. Eng. Chem. 1959, 51 (9), 993–996

[2] H. M. Torres Galvis, J. H. Bitter, C. B. Khare, M. Ruitenbeek, A. I. Dugulan, K. P. de Jong, Science 2012, 335, 835-838

[3] E. de Smit, B. M. Weckhuysen, Chem. Soc. Rev. 2008, 37, 2758-2781

[4] Xu, J.-D. et al, Appl. Catal. A Gen. 2015, 514, 103–113

[5] H.M. Torres Galvis, J.H. Bitter, T. Davidian, M. Ruitenbeek, A.I. Dugulan, K.P. de Jong, J. Am. Chem. Soc. 2012, 134, p. 16207-16215

[6] B. Wu et al., Fuel 2004, 83, 205–212

[7] A.L. Chaffee, I. Campbell, N. Valentine, Applied catalysis, 1989, 47, 253-276

[8] H. Xiong, M.A. Motchelaho, M. Moyo, L.L. Jewell, N.J. Coville, Fuel 2015, 150, 687-696

[9] H.M. Torres Galvis, A.C.J. Koeken, J.H. Bitter, T. Davidian, M. Ruitenbeek, A.I. Dugulan, K.P.de Jong, Journal of Catalysis 2013, 303, 22-30

[10] Z. Tao, Y. Yang, H. Wan, T. Li, X. An, H. Xiang, Y. Li, Catalysis Letters 2007, 114, 161-168

[11] F. Fischer, H. Tropsch, Berichte der deutschen chemischen Gesellschaft 1926, 59 (4), 832–836

[12] M.E. Dry, Journal of Chemical Technology and Biotechnology 2001, 77, 43-50

[13] C. Wang, L. Xu, Q. Wang, Journal of Natural Gas Chemistry 2003, 12, 10-16

[14] R.W. Dorner, D.R. Hardy, F.W. Williams, H.D. Willauer, Energy envion. Sci. 2010, 3, 884-890

[15] J. Haber, J.H. Block, B. Delmon, Pure & Appl. Chem. 1995, 67, 1261

[16] R.E. Wolf, What is ICP-MS? and more importantly, what can it do?, 2005

[17] Shriver & Atkins', Inorganic Chemistry, fifth edition, 2010, 247-248

[18] K. Czerwinski, Lecture 22: Thermal methods, 2005 http://radchem.nevada.edu/classes/chem455/lecture_22__thermal_methods.htm

[19] K. Thet, N. Woo, Gas Chromatography, 2016 http://chemwiki.ucdavis.edu/Core/Analytical_Chemistry/Instrumental_Analysis/Chromatography/Gas_Chromatography

[20] S. Chen, Y. Xin, Y. Zhou, F. Zhang, Y. Ma, H. Zhou, L. Qi, Journal of Materials Chemistry A 2014, 2, 15582-15589

[21] H.A. Asmaly, B. Abussaud, Ihsanullah, T.A. Saleh, V.K. Gupta, M.A. Atieh, Journal of Saudi Chemical Society 2015, 19, 511-520

[22] D.M. Crumpton, R.A. Laitinen, J. Smieja, D.A. Cleary, Journal of Chemical Education 1996, 73 (6), 590-591